

# Tristability in a non-equilibrium double-quantum-dot in Kondo regime

Gustavo. A. Lara <sup>1</sup>, Pedro A. Orellana <sup>2</sup> and Enrique V. Anda <sup>3</sup>

<sup>1</sup>*Departamento de Física, Universidad de Antofagasta,  
Casilla 170, Antofagasta, Chile.*

<sup>2</sup>*Departamento de Física, Universidad Católica del Norte,  
Casilla 1280, Antofagasta, Chile.*

<sup>3</sup>*Departamento de Física, P. U. Católica do Rio de Janeiro,  
C.P. 38071-970, Rio de Janeiro, RJ, Brazil.*

Electron tunneling through a non-equilibrium double quantum dot in the Kondo regime is studied. In the region of negative differential resistance, it is shown that this system possesses a complex response to the applied potential characterized by a tristable solution for the current. Increasing the applied potential or reducing the inter-dot coupling, the system goes through a transition from a coherent inter-dot regime to an incoherent one. The different nature of the solutions are characterized and it is shown that the effects of the asymmetry in the dot-lead coupling can be used to control the region of multistability. The mean-field slave-boson formalism is used to obtain the solution of the problem.

The Kondo effect in quantum-dots (*QDs*) has been extensively studied in the last years.<sup>1,2</sup> The experimental evidence has confirmed that many of the phenomena that characterize strongly correlated metals and insulators, as it is the case of the Kondo effect, are present in *QDs*. The *QDs* allow to study systematically the quantum-coherence many-body Kondo state, due to the possibility of continuous tuning of the relevant parameters governing the properties of this state, in equilibrium and non-equilibrium situations.

The electron tunneling through double-quantum-dots (*DQD*) in the Kondo regime has received much attention in recent years.<sup>4-12</sup> In comparison with a single quantum-dot, the double-quantum-dot has a richer physics. For example in *DQDs* it is possible to study the competition between the inter-dot antiferromagnetic spin-spin correlation and the dot-conduction spin-spin correlation present in its ground state and also it can be investigated the inter-dot coherence effects that results from the Coulomb interaction. The type of coupling between the *QDs* determines the character of the electronic states and the transport properties of the artificial molecule. In the tunneling regime, the electronics states are extended across the entire system and can be constructed from a coherent state based on the bonding or anti-bonding levels of the *QDs*. Some aspects of the non-equilibrium transport properties of a simplified *DQD* in the Kondo regime, constituted by two identical *QDs* has recently been studied<sup>11</sup>. When the inter-dot coupling is greater than the level broadening, there is a region of voltage where this system shows a bistable behavior characterized by two solutions for the current. This behavior re-

sembles the *J-V* characteristic curve of a double barrier structure in the accumulation of charge regime and in doped superlattices.<sup>13,18-21</sup> However, theoretical and experimental studies have confirmed that a double barrier structure possesses a more complex behavior than the one predicted by a bistability. The *J-V* curve of this system has in many cases a Z-shape, indicating the existence of a tristable solution for the current.<sup>14</sup>

In this work we analyze the new physics derived from the complex behavior that characterize the electron tunneling through a non-equilibrium *DQD* in the Kondo regime. Although this system is essentially different from a double barrier heterostructure, we find that, in certain region of the parameter space, the *J - V* characteristic curve of both are similar. However, the problem we analyze has much richer physics. Increasing the asymmetry of the coupling of the dots with the leads or reducing the inter-dot coupling, the system goes through a transition from a coherent inter-dot regime to an incoherent one. The characteristic curve reflects this transition changing from a Z-shape in the incoherent region to a loop-shape when the dots behave coherently. The different nature of the solutions are characterized and it is shown that the effects of the asymmetry in the dot-lead coupling can be used to control the region of multistability.

We adopt the two-fold degenerate Anderson Hamiltonian in the limit  $U \rightarrow \infty$ , that is diagonalized using the mean-field slave-boson formalism. Although this mean-field approximation has, in certain region of the parameters that define the system, a non-physical solution it has been shown that the physics related to the negative differential resistance is not associated to it<sup>11</sup>. The *DQD* is driven out-of-equilibrium by means of a dc bias voltage  $V$  at zero temperature. The double occupancy in each dot is forbidden and the inter-dot Coulomb interaction neglected. We introduce the slave-boson operator  $b_\alpha^\dagger$  that creates an empty state and a fermion operator  $f_{\alpha\sigma}$  that annihilates a single occupied state with spin  $\sigma$ . To eliminate the possibility of double occupancy we impose the constraint  $Q_\alpha \equiv \sum_\sigma f_{\alpha\sigma}^\dagger f_{\alpha\sigma} + b_\alpha^\dagger b_\alpha = 1$ . The annihilation operator of an electron in the dot  $\alpha$  is  $c_{\alpha\sigma} = b_\alpha^\dagger f_{\alpha\sigma}$ . In the mean field approximation the bosonic operators  $b_\alpha^\dagger$  and  $b_\alpha$  are replaced by their expectation values,  $\langle b_\alpha \rangle = \tilde{b}_\alpha \sqrt{2} = \langle b_\alpha^\dagger \rangle = \tilde{b}_\alpha^\dagger \sqrt{2}$ . Hence

the Hamiltonian of the double quantum-dot connected to leads plus constraints is written as,

$$H = H_{lead} + \sum_{\alpha=0,1,\sigma} \tilde{\varepsilon}_\alpha n_{\alpha\sigma} + \tilde{V}_L \sum_{\sigma} (c_{-1\sigma}^\dagger f_{0\sigma} + f_{0\sigma}^\dagger c_{-1\sigma}) + \tilde{V}_R \sum_{\sigma} (f_{1\sigma}^\dagger c_{2\sigma} + c_{2\sigma}^\dagger f_{1\sigma}) + \tilde{t}_c \sum_{\sigma} (f_{0\sigma}^\dagger f_{1\sigma} + f_{1\sigma}^\dagger f_{0\sigma}) + \sum_{\alpha=0,1} \lambda_\alpha (\tilde{b}_\alpha^\dagger \tilde{b}_\alpha - 1). \quad (1)$$

where  $\tilde{\varepsilon}_0 = \varepsilon_0 + \lambda_0$ ,  $\tilde{\varepsilon}_1 = \varepsilon_1 + \lambda_1$ ,  $\tilde{V}_L = V_L \tilde{b}_0$ ,  $\tilde{V}_R = V_R \tilde{b}_1$ ,  $\tilde{t}_c = t_c \tilde{b}_0 \tilde{b}_1$ , the  $\lambda_\alpha$  are Lagrangian multipliers which guarantee the constraint conditions on the  $Q_\alpha$  and the parameters  $t_c$ ,  $V_L$  and  $V_R$  are the inter-dot connection and left and right dot connections with the leads respectively.

The first term on the right-hand side of Eq.1 represents the electrons in the left and right leads;

$$H_{lead} = \sum_{i \neq 0,1} \varepsilon_i n_{i\sigma} + t \sum_{\langle ij \neq 0,1 \rangle \sigma} c_{i\sigma}^\dagger c_{j\sigma}. \quad (2)$$

where the operator  $c_{i\sigma}^\dagger$  creates an electron in the site  $i$  with spin  $\sigma$ ,  $\varepsilon_i$  is the site energy and  $t$  is first-neighbor hopping in the leads.

Here  $H_{lead}$  corresponds to the free-particle Hamiltonian with eigenfunctions of the Bloch type,

$$|k, \sigma\rangle = \sum_j e^{ikja} |j, \sigma\rangle \quad (3)$$

where  $|k, \sigma\rangle$  is the momentum eigenstate with spin  $\sigma$  and  $|j\rangle$  is a Wannier state localized at site  $j$  of spin  $\sigma$ . The dispersion relation associated with these Bloch states reads

$$\varepsilon_k = 2t \cos(ka) \quad (4)$$

The model has an energy band, extending from  $-2t$  to  $+2t$ , with the first Brillouin zone expanding the  $k$  interval  $[-\pi/a, \pi/a]$ .

The stationary state of the complete Hamiltonian  $H$  with energy  $\varepsilon_k$  can be written as

$$|\psi_{k\sigma}\rangle = \sum_j a_{j\sigma}^k |j, \sigma\rangle \quad (5)$$

where the coefficients  $a_{j\sigma}^k$  are given by,

$$a_{j\sigma}^k = \langle j, \sigma | \psi_{k\sigma} \rangle. \quad (6)$$

We obtain the following eigenvalue equations for the Wannier amplitudes  $a_{j\sigma}^k$

$$\begin{aligned} \varepsilon_k a_{j,\sigma}^k &= \langle j, \sigma | H | \psi_{k\sigma} \rangle \\ \varepsilon_k a_{j,\sigma}^k &= \varepsilon_j a_{j,\sigma}^k + t(a_{j-1,\sigma}^k + a_{j+1,\sigma}^k) \quad (j \neq -1, 0, 1, 2), \\ \varepsilon_k a_{-1(2),\sigma}^k &= \varepsilon_{-1(2)} a_{-1(2),\sigma}^k + \tilde{V}_{L(R)} a_{0(1),\sigma}^k + t a_{-2(3),\sigma}^k, \\ \varepsilon_k a_{0(1),\sigma}^k &= \tilde{\varepsilon}_{0(1)} a_{0(1),\sigma}^k + \tilde{V}_{L(R)} a_{-1(2),\sigma}^k + \tilde{t}_c a_{1(0),\sigma}^k, \end{aligned} \quad (7)$$

where  $a_{j,\sigma}^k$  is the amplitude of probability to find the electron in the site  $j$  and state  $k$  with spin  $\sigma$ .

The four parameters ( $\tilde{b}_0$ ,  $\tilde{b}_1$ ,  $\lambda_0$ ,  $\lambda_1$ ) are determined minimizing the expectation values of the Hamiltonian (7). They satisfy the set of four equations:

$$\begin{aligned} \tilde{b}_{0(1)}^2 + \frac{1}{2} \sum_{k,\sigma} |a_{0(1),\sigma}^k|^2 &= \frac{1}{2}, \\ \frac{\tilde{V}_{L(R)}}{2} \sum_{k,\sigma} \text{Re}(a_{-1(2),\sigma}^{k*} a_{0(1),\sigma}^k) + \\ \frac{\tilde{t}_c}{2} \sum_{k,\sigma} \text{Re}(a_{1(0),\sigma}^{k*} a_{0(1),\sigma}^k) + \tilde{\lambda}_{0(1)} \tilde{b}_{L(R)}^2 &= 0. \end{aligned} \quad (8)$$

The sum over the wave vector  $k$  covers all the occupied states. The resulting equations are nonlinear because of the renormalization of the localized levels in the dots, the interdot coupling tunneling and the coupling tunneling between the QDs and the leads.

The stationary scattering problem is solved by finding the eigenstates with positive  $k$ . In order to study the solutions of equations (4) and (5) we assume a plane wave incident from the left with an amplitude  $I$ , with a partial reflection amplitude  $R$ . The waveform at the right is a simple plane wave with intensity given by the transmission amplitude  $T$ . Taking this to be the solution of the system, we can write,

$$\begin{aligned} a_j^k &= I e^{ikaj} + R e^{-ikaj}, \quad j < 0 \\ a_j^k &= T e^{ikRaj}, \quad j > 1 \end{aligned} \quad (9)$$

and those with negative  $k$

$$\begin{aligned} a_j^{-k} &= \tilde{I} e^{-ikaj} + \tilde{R} e^{ikaj}, \quad j > 1 \\ a_j^{-k} &= \tilde{T} e^{-ikLaj}, \quad j < 0 \end{aligned} \quad (10)$$

These functions describe plane-wave electron approaching the scattering potential from  $j = -\infty$  and  $j = +\infty$ , respectively, with transmission and reflection amplitudes  $T$  and  $R$  for  $k > 0$ , and  $\tilde{T}$  and  $\tilde{R}$  for  $k < 0$ .

The solution of equations (7) can be obtained through an adequate iteration from right to left for  $k > 0$ , and from left to right for  $k < 0$ . For a given transmitted amplitude, the associated reflected and incident amplitudes may be determined by matching the iterated function to the proper plane wave at the left lead for  $k > 0$  and at the right lead for  $k < 0$ . The transmission amplitude  $t(k) = T/I$  and  $\tilde{t}(k) = \tilde{T}/\tilde{I}$  are obtained from the iterative procedure.

The equations (7) and (8) are nonlinear and require a self-consistent solution that is obtained using a conjugate gradient algorithm. In this work, we are interested in analyzing all the stationary solutions for the current. As  $J(V)$  and  $V(J)$  are multivalued functions, the multiple solutions for the quantities  $\tilde{b}_0$ ,  $\tilde{b}_1$ ,  $\lambda_0$ ,  $\lambda_1$  are obtained by fixing, first the external potential  $V$  and afterwards the current  $J$  in the equations of motion of the

system. This method permits us to obtain the complete  $J$ - $V$  characteristic curve.

Once the amplitudes  $a_{j,\sigma}^k$  are known, the current is numerically obtained from,

$$J = \frac{2e}{\hbar} \tilde{V}_L \sum_{k,\sigma} \text{Im}\{a_{-1,\sigma}^{k*} a_{0,\sigma}^k\}. \quad (11)$$

We study first a model which consists of two leads equally connected ( $V_L = V_R = V_0$ ) to two quantum dots with  $\mu_L = -V/2$  and  $\mu_R = V/2$ ,  $t = 30 \Gamma_0$ ,  $V_0 = 5.48 \Gamma_0$ ,  $\varepsilon_0 = \varepsilon_1 = -3.5 \Gamma_0$  (Kondo regime with  $T_K \approx 10^{-3} \Gamma_0$  with  $\Gamma_0 = 2\pi V_0^2 \rho(0)$ ).

The Fig 1 shows the  $J$ - $V$  characteristic curve for different values of  $t_c$ . Within a range of the external bias voltage values, there are three stationary solutions for the current. We can identify two regimes. One for  $\Gamma_0 < t_c < t_{c0}$ , ( $t_{c0}$  is a constant to be analyzed below), where the  $J - V$  characteristic curve has a Z-shape and another one for  $t_c > t_{c0}$  where the curve becomes loop-shaped. An experiment that would consist in studying this system just by simply continuously modifying the applied potential  $V$  would characterize the behavior of the current as bistable. At a critical value  $V_{c\uparrow}$ , there would be a discontinuous reduction of the current when  $V$  is increased and other  $V_{c\downarrow}$  ( $V_{c\uparrow} > V_{c\downarrow}$ ) where the current would rise, ( $t_c < t_{c0}$ ), or diminish, ( $t_c > t_{c0}$ ), discontinuously when  $V$  is reduced. In this case the interior of the bistability remains inaccessible to the experiment. However, the internal shape could be reached, as it is for the case of double barrier heterostructures, employing a load line in the experimental measurement that permits to go along all the points of the  $J - V$  characteristic curve.

When  $t_c > \Gamma_0$ , the Kondo levels  $\tilde{\varepsilon}_0$  and  $\tilde{\varepsilon}_1$  are splitted into two molecular states, corresponding to the bonding and antibonding levels. They are located in,  $\tilde{\varepsilon}_{\pm} = \{(\tilde{\varepsilon}_0 + \tilde{\varepsilon}_1)/2 \pm \sqrt{(\tilde{\varepsilon}_0 - \tilde{\varepsilon}_1)^2 + 4\tilde{t}_c^2}\}/2$ . In the Fig. 2a and 2b we plot  $\tilde{\varepsilon}_{\pm}$ , as a function of  $V$ , for two values of  $t_c$ . The main features are: a) For  $V = 0$ , the bonding and antibonding levels satisfies  $\tilde{\varepsilon}_{\pm} = \pm \tilde{t}_c$ . When the bias  $V$  is increased of the order of  $T_k$ ,  $\tilde{\varepsilon}_{\pm}$  are kept almost constant and the dots reacts to the external potential in a coherent way. For higher values of  $V$ ,  $\tilde{\varepsilon}_+$  and  $\tilde{\varepsilon}_-$  approach each other and go through the multistable region. The right dot is connected to the left reservoir by the mediation of the left one through an effective interaction  $V_L^{eff}$  that for energies in the vicinity of the Fermi level of the order of  $T_k$ , is approximately given by  $V_L^{eff} = \tilde{t}_c/2\pi\tilde{V}_L\rho(0)$ . The effective levels have a clear different behavior whether the right dot is interacting stronger with the left than with the right  $V_L^{eff} > \tilde{V}_R$  or the contrary,  $V_L^{eff} < \tilde{V}_R$ . For the case we are analyzing, ( $V_L = V_R = V_0$ ), this can be controlled manipulating the value of  $t_c$ . Defining  $t_{c0}$  as the frontier between these two situation, in the case when  $t_c < t_{c0}$ , increasing the potential beyond the multistable region, the coherence between the dots is lost and  $\tilde{\varepsilon}_+$  and

$\tilde{\varepsilon}_-$  converge towards their own chemical potential  $\mu_{L(R)}$ , as display in Fig.2a. The interactions of the dots with the leads  $\tilde{V}_L$  and  $\tilde{V}_R$  are equally renormalized as can be seen in Fig 2c. The system possesses an splitted Kondo peak. One sub-peak with its weight essentially located at the left dot with energy at the neighborhood of  $\mu_L$  and the other located at the right dot near  $\mu_R$ . For  $t_c > t_{c0}$  by the contrary, due to the stronger interaction between the dots, they maintain their coherence and result to be partially disconnected from the right lead. This is reflected in the behavior of the renormalized interaction of each dot with its respective lead as shown in Fig.2d and in their localized levels  $\tilde{\varepsilon}_+$  and  $\tilde{\varepsilon}_-$ , that both follow  $\mu_L$  as  $V$  increases presented in Fig2b. The Kondo peak, almost pinned at  $\mu_L$ , is in this case equally distributed among the two dots.

Next we will discuss the effect of the asymmetric site energies case,  $\varepsilon_0 \neq \varepsilon_1$ . We model the asymmetric site energies by setting  $\varepsilon_0 = (1 - \kappa)e_0$ ,  $\varepsilon_1 = (1 + \kappa)e_0$ , where  $\kappa$  is the asymmetry parameter and  $e_0 = -3.5 \Gamma_0$ . Figs 3 shows the  $J$ - $V$  characteristics for various values of  $\kappa$  at  $t_c = 1.3\Gamma_0$  and  $t_c = 2.5\Gamma_0$ . It is seen that the region of multistability is very sensitive to the change of  $\kappa$  and in particular it disappears for sufficiently large values of it. The coherent or incoherent behavior of the dots discussed above can be controlled in this case changing the asymmetry parameter  $\kappa$ . Fig 4 shows a map with the regions of multistability depending on the bias voltage  $V$  and  $\kappa$ . It is seen that the width of the multistability region has lower and upper limits, which depend upon the asymmetry in the dot-lead coupling. Similar results were obtained for an asymmetric dot-lead coupling case,  $V_L \neq V_R$ .

In this paper we have studied the  $J$ - $V$  characteristic curve of a double-quantum-dot in the Kondo regime. It exhibits a multistable behavior that enhances as the interdot coupling tunneling increases. It becomes Z-shaped or loop-shaped depending on the various coupling tunneling parameters, which control whether the dots respond coherently or incoherently to the external applied potential. Moreover, we show that it is possible to manipulate the multistability in a sample by changing the asymmetry in the dot-lead coupling.

Work supported by grants Milenio ICM P99-135-F, FONDECYT 1990443, Cátedra Presidencial en Ciencias, Fundación Antorchas/Vitae/Andes, FINEP and CNPq.

<sup>1</sup> D.Goldhaber-Gordon et al., Nature (London) **391**, 156 (1998); Phys. Rev. Lett. **81**, 5225 (1998).

<sup>2</sup> Sara M. Cronenwett, Tjerk H. Oosterkamp and Leo P. Kouwenhoven, Science **281**, 540 (1998).

<sup>3</sup> T.K. Ng and P.A. Lee, Phys. Rev. Lett. **61**, 1768 (1988), L.I. Glazman and M.E. Raikh, JETP. Lett. **47**, 452 (1988).

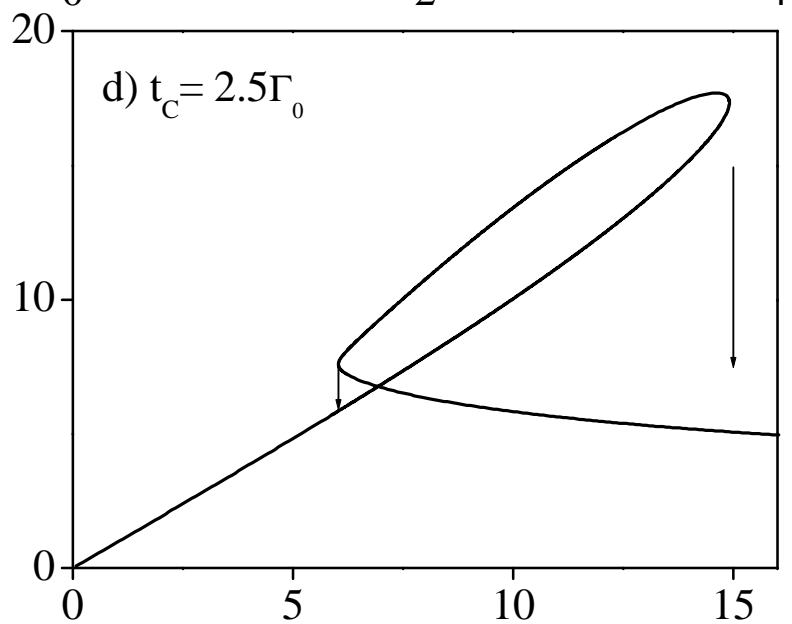
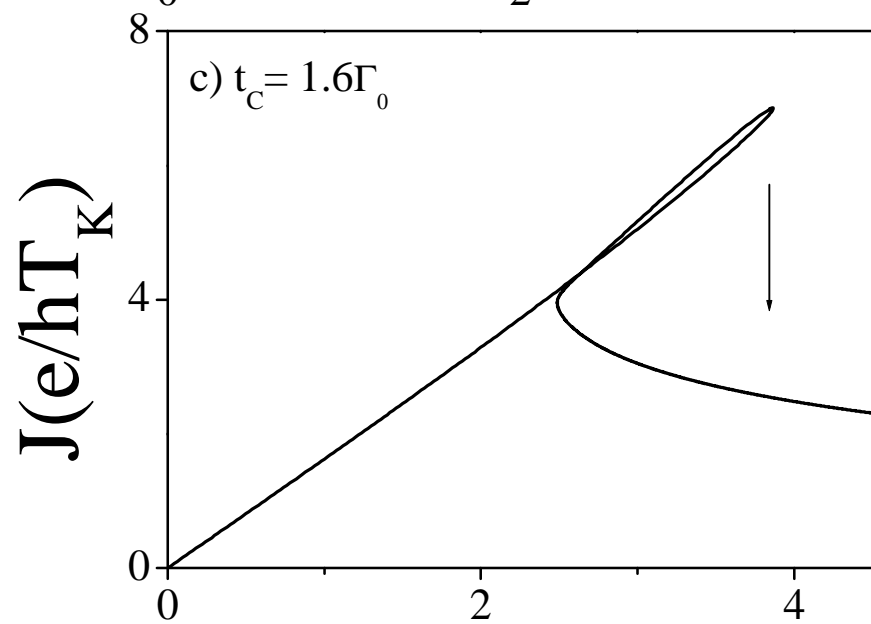
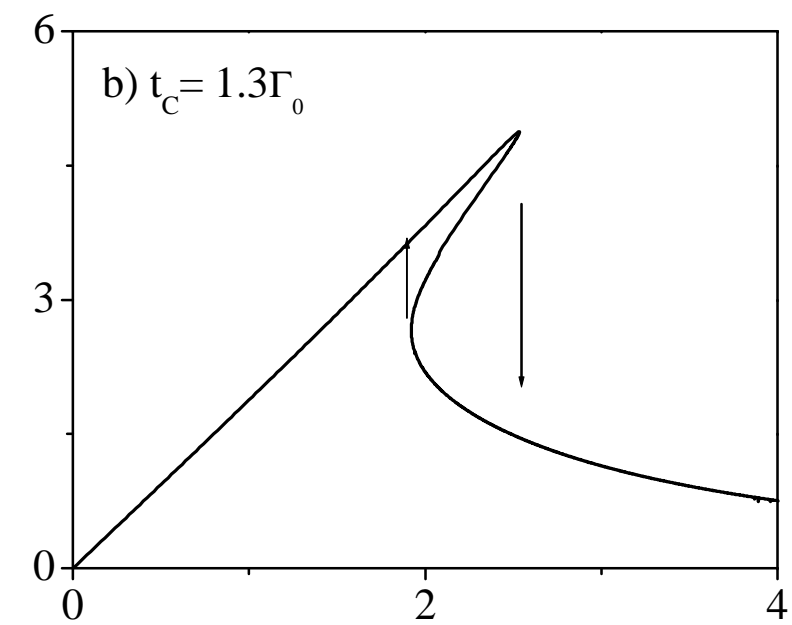
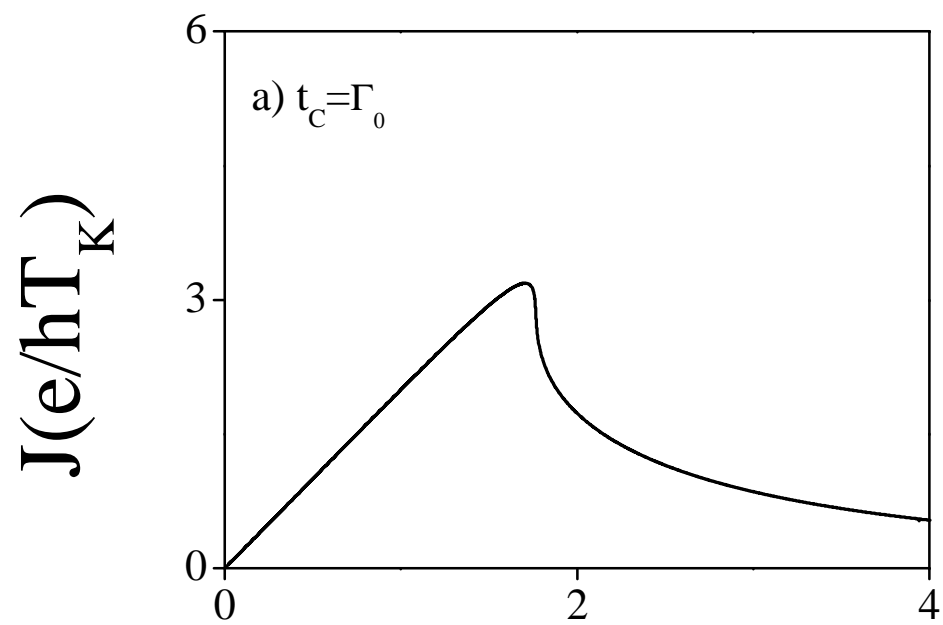
- <sup>4</sup> H. Jeong, A.M. Chang and M.R. Melloch, Science **293** 2221 (2001).
- <sup>5</sup> R.Aguado and D.C. Langreth Phys.Rev.Lett. **85**,1946 (2000).
- <sup>6</sup> Antoine Georges and Yigal Meir, Phys. Rev. Lett. **82**, 3508 (1999).
- <sup>7</sup> C.A. Busser, E.V. Anda, A.L. Lima, M. A.Davidovich and G. Chiappe, Phys. Rev. B **62**, 9907 (2000).
- <sup>8</sup> Tomosuke Aono and Mikio Eto, Phys. Rev. B **63**,125327 (2001).
- <sup>9</sup> Wataru Izumida and Osamu Sakai, Phys. Rev. B **62** 10260 (2000).
- <sup>10</sup> T. Ivanov Europhys. Lett. **40**, 183 (1997).
- <sup>11</sup> P.A. Orellana, G.A. Lara, E.V. Anda, cond-mat/0107487 (To appear in Phys. Rev. B).
- <sup>12</sup> Bing Dong and X.L. Lei, cond-mat/0112500 (2001).
- <sup>13</sup> V.J. Goldman, D.C.Tsui and J.E. Cunningham, Phys. Rev. Lett. **58**, 1256 (1987).
- <sup>14</sup> A.D Martin, M.K.F. Lerch, P.E. Simmonds and E. Eaves, Appl. Phys. Lett. **64**, 1248 (1994).
- <sup>15</sup> S.E. Barnes, J. Phys. F **6**, 1375 (1976); **7**, 2637 (1977).
- <sup>16</sup> P. Coleman, Phys. Rev. B **29**, 3035 (1984); **35**, 5072 (1987).
- <sup>17</sup> N. Read and D.M. Newns, J. Phys. C, 3273 (1983); Adv. Phys. **36**, 799 (1988).
- <sup>18</sup> F. Prengel, A. Wacker, and E. Scholl, Phys. Rev. B **50**, 1705 (1994).
- <sup>19</sup> J. Kastrup, R. Hey, K. H. Ploog, H. T. Grahm, L. L. Bonilla, M. Kindelan, M. Moscoso, A. Wacker, and J. Galán, Phys. Rev. B **55**, 2476 (1997).
- <sup>20</sup> R. Aguado, G. Platero, M. Moscoso, and L. L. Bonilla, Phys. Rev. B **55**, R16053 (1997).
- <sup>21</sup> P.L Pernas, F. Flores and E.V. Anda, Phys. Rev. B **47**, 4779 (1993).
- <sup>22</sup> B.A. Jones, B.G. Kotliar, A. J. Millis, Phys. Rev. B **39**, R3415 (1989).
- <sup>23</sup> S.Sasaki, S. De Franceschi, J.M. Elzerman, W.G. van de Wiel, M. Eto, S. Tarucha and L. P. Kowenhoven, Nature **405**, 764 (2000).

FIG. 1.  $J$ - $V$  curve for a)  $t_c = \Gamma_0$ , b)  $t_c = 1.3\Gamma_0$ , c)  $t_c = 1.6\Gamma_0$  and d)  $t_c = 2.5\Gamma_0$

FIG. 2. Figures 2 a) and 2 b) level energies  $\epsilon_{\pm}$  vs  $V$  at  $t_c = 1.3\Gamma_0$   $t_c = 1.6\Gamma_0$  respectively. Figures 2 c) and d) the corresponding renormalization of the dot lead coupling

FIG. 3.  $J$ - $V$  curve for the asymmetric site energies case at a)  $t_c = 1.3\Gamma_0$  with  $\kappa=0.005$  (solid line), 0.015 (dash line), 0.04 (dot line) and 0.06(short-dash line), b)  $t_c = 2.5\Gamma_0$  with  $\kappa=0.04$  (solid line), 0.08 (dash line), 0.12 (dot line) and 0.16(short-dash line)

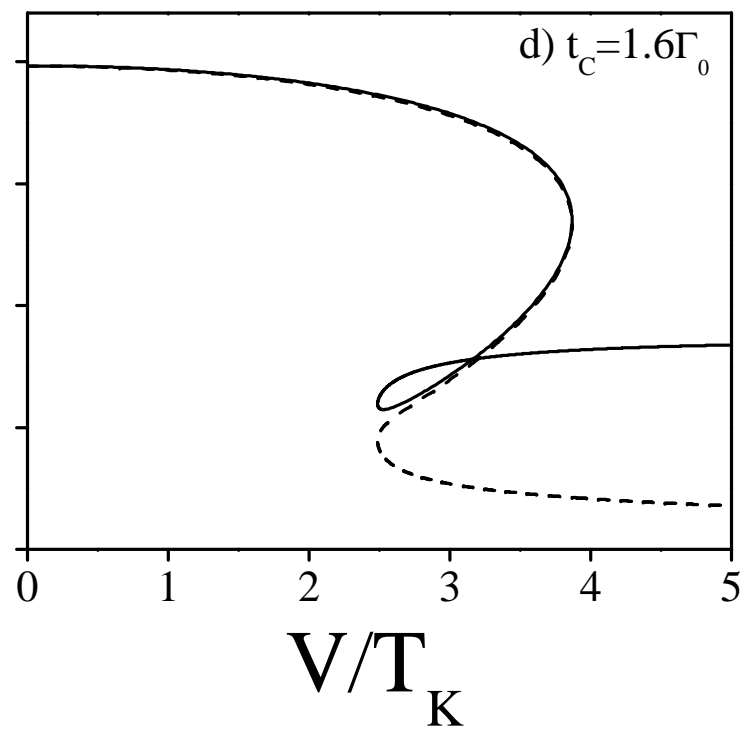
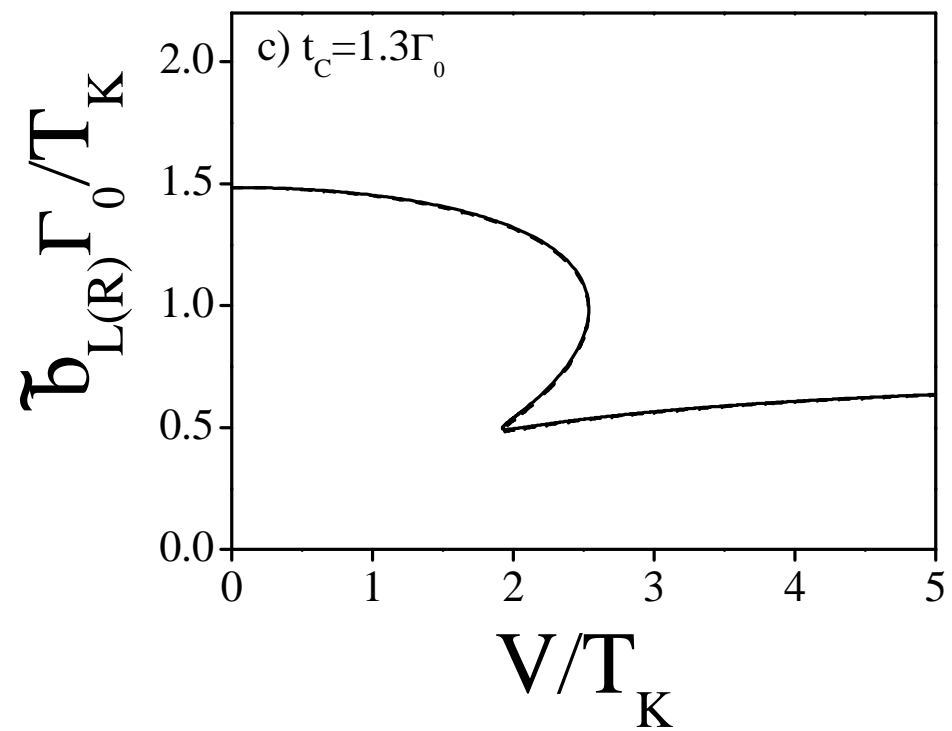
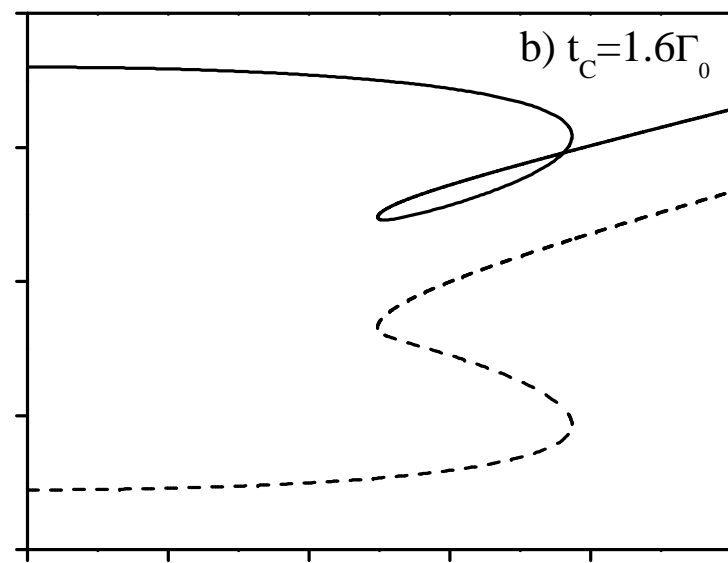
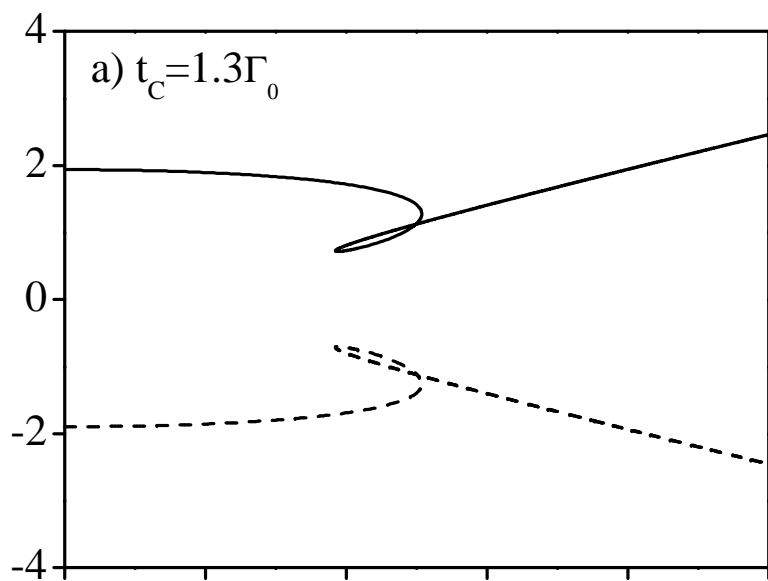
FIG. 4. Map  $V$  versus  $\kappa$  at a)  $t_c = 1.1\Gamma_0$ , b)  $t_c = 1.2\Gamma_0$ , c)  $t_c = 1.6\Gamma_0$ , d)  $t_c = 2.5\Gamma_0$

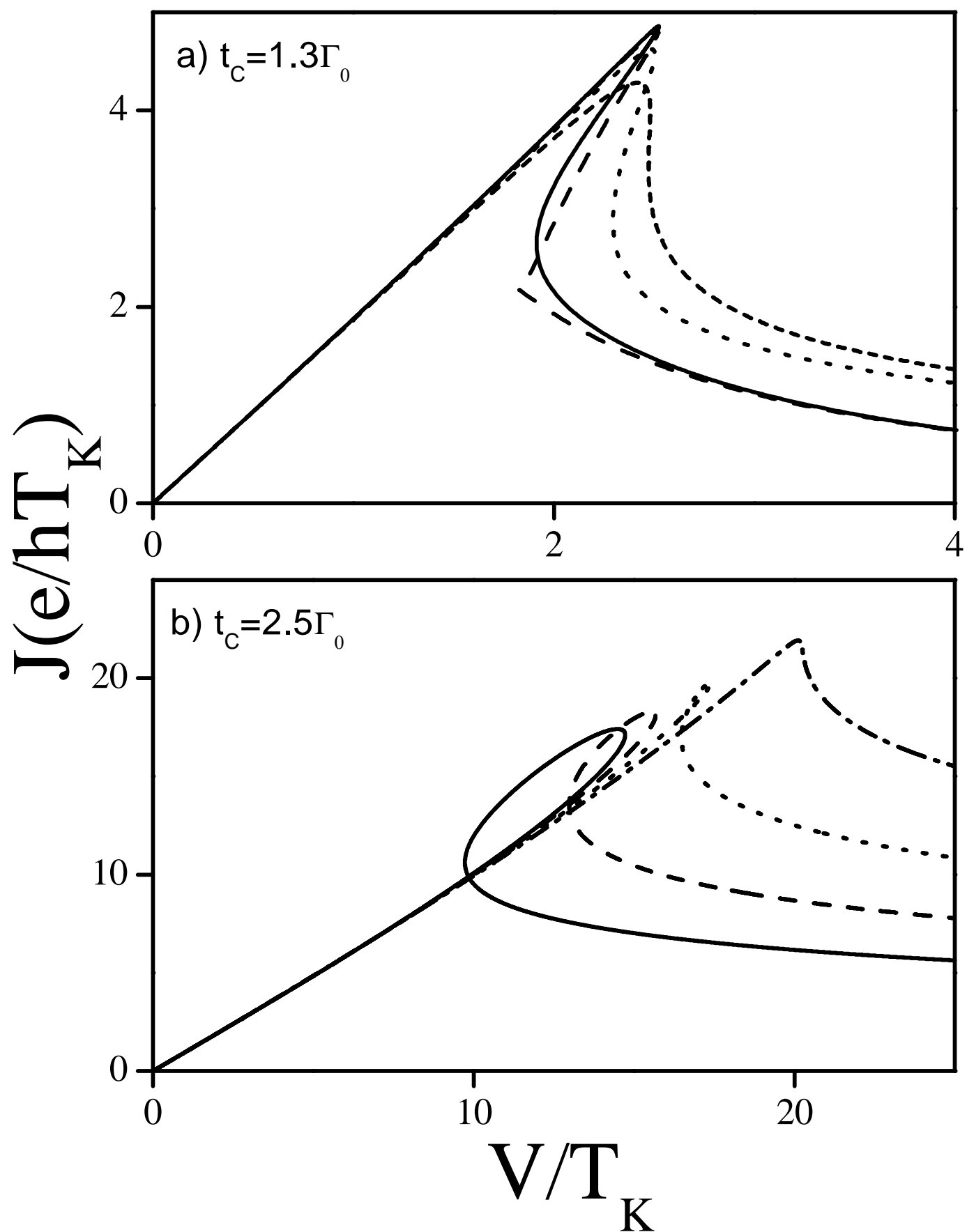


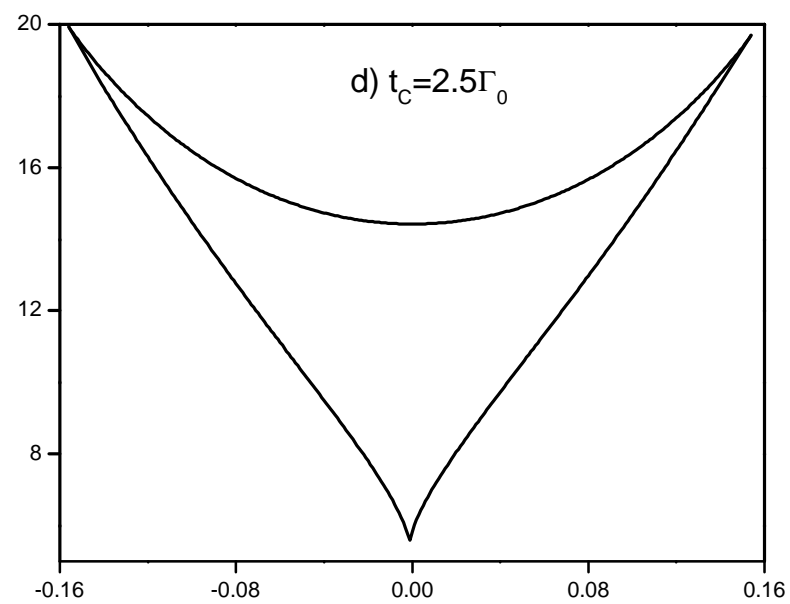
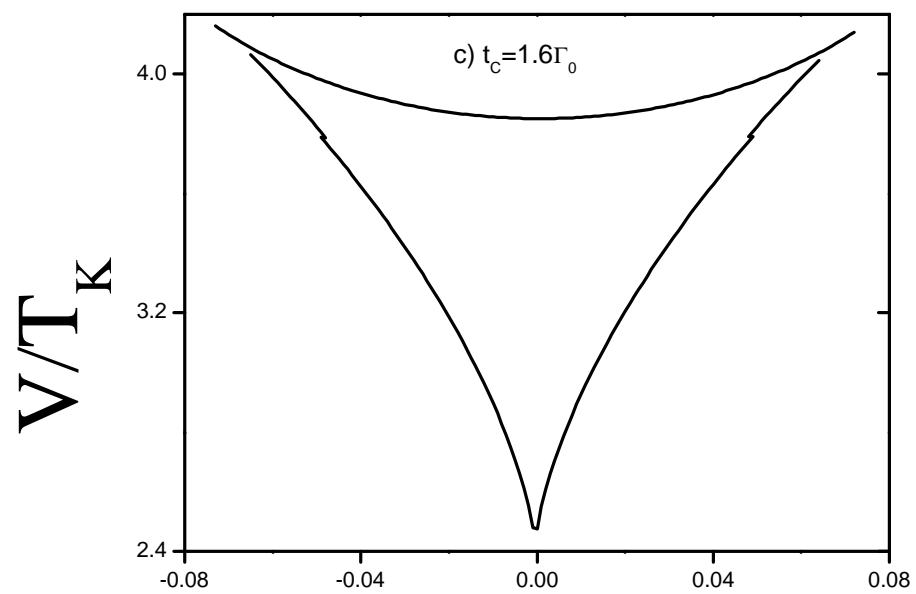
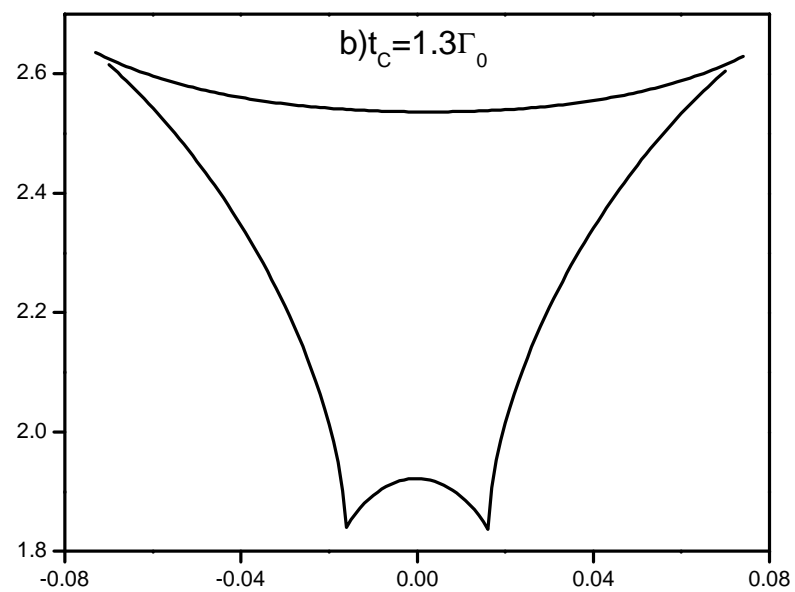
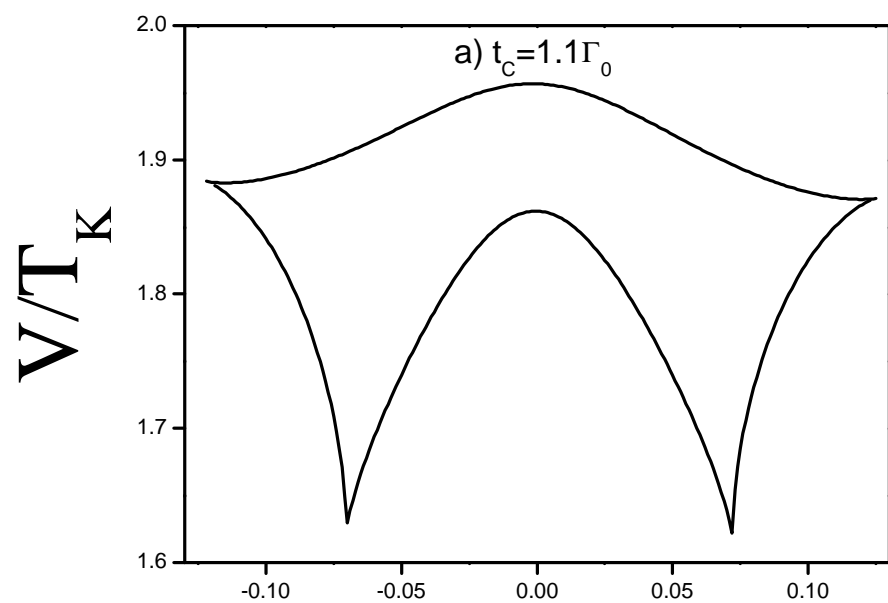
$V/T_K$

$V/T_K$

level position( $T_K$ )







$K$

$K$